

# A Study of Semi-Active Vibration Control for Vehicle Suspension System Using an Adjustable Shock Absorber

Jian-Da Wu<sup>1,\*</sup>, Chih-Jer Lin<sup>2</sup> and Kun-Yin Kuo<sup>1</sup>

<sup>1</sup>Graduate Institute of Vehicle Engineering, National Changhua University of Education, 1 Jin-De Rd., Changhua City, Changhua 500, Taiwan

<sup>2</sup>Department of Mechanical and Automation Engineering, Da-Yeh University, 112 Shan-Jeau Road, Da-Tsuen, Changhua 515, Taiwan

Received 24th November 2007

## ABSTRACT

A semi-active vehicle suspension system using an adjustable shock absorber for a quarter-car model vibration control is presented in this paper. Two control techniques are developed for assessing both ride comfort and road handling. Apart from the conventional proportional-integral-derivative (PID) controller, a controller using fuzzy sets and fuzzy inferences is developed and its performance is experimentally tested. In the preliminary work, the characteristics and performance of an adjustable shock absorber are measured in order to build a data bank on various road conditions. The experimental results indicated that both the PID controller and the fuzzy controller effectively suppress the vibration of the proposed quarter-car model. The comparison and analysis of the proposed controllers are also described in this paper. Furthermore, the characteristic analysis and evaluation of the human exposure to whole body vibration has also been established by international standard.

*Keywords.* Semi-active vibration control; vehicle suspension system; adjustable shock absorber.

## 1. INTRODUCTION

A vehicle suspension system is used to improve ride comfort and road handling by controlling the relative position and motion between vehicle body and wheels. Generally, vehicle suspension systems can be classified into three categories, passive, semi-active active as shown in Fig. 1. Passive suspension is the common suspension system for vehicles. It can only temporarily dissipate perturbations by springs and damping, without energy supplied by the suspension system. Therefore, a fixed suspension setting has to cope with a wide variety of road conditions. Similarly, a semi-active control strategy does not provide any energy into suspension system. It has an adjustable damper which is the only difference between semi-active and passive suspension systems. The damper might change its damping characteristics continuously in response to the body motion sensed. Hence, the performance of a semi-active suspension system should be better than that of a passive suspension system. An active suspension system has the ability to store, dissipate and provide energy to the system. It uses sensors to measure vehicle performance such as vertical vehicle body acceleration and vertical wheel acceleration and then generates force to control not only the vehicle attitude but also the wheel motions by an actuator. Although the active suspension system provides better control performance than the semi-active suspension system, it has a major

---

Corresponding author: E-mail address: jdwu@cc.ncue.edu.tw

## A Study of Semi-Active Vibration Control for Vehicle Suspension System Using an Adjustable Shock Absorber

drawback in that it requires considerable external power together with increased complexity and cost, and decreased reliability. The semi-active suspension combines the advantages of both active and passive suspensions. Hence, the system has become a popular suspension system and many control strategies are presented.

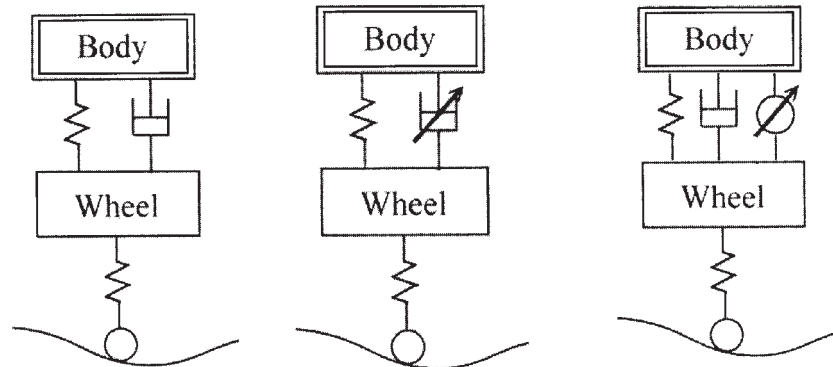


Figure 1. Three categories of suspension system. (a) passive suspension system (b) semi-active suspension system (c) active suspension system

With the rapid development of vehicles' performance the shock absorber will become more important than ever for ride quality. In 1959, Jackson G.W [1] presented a performance test method for the shock absorber. Moreover, the shock absorber damping force and spring constant can now be adjusted to meet driver preferences. Therefore, many techniques and design procedures have been proposed to improve the characteristics of suspension systems. In 1990, Satoh et al. [2] analysed the hydraulic system functions required in an active suspension built with an electro-hydraulic pressure control system. Simulations and actual vehicle tests are presented to show how these features enable this active suspension to provide superior performance. In 2002, Yao et al. [3] proposed a method of semi-active control of a vehicle suspension system with a magneto-rheological (MR) damper and tested the performance of the damper. The response of the MR vehicle suspension proved that it provided excellent performance by changing the damping. In 2003, a control scheme for a suspension system using a neural network controller was proposed by S. Yildirim [4].

In recent years, numerous studies [5-7] based on "skyhook" theory have developed the control logic for semi-active suspension systems. The skyhook damper control provides four conditions to change the damping coefficients in accordance with the body and suspension velocity. Stability and optimality are the most important requirements for any control suspension system. Most of the present works on the stability analysis are based on fuzzy logic. The fuzzy logic based controller for the semi-active suspension system was proposed by a number of workers[8-10].

In the present study, a control system using fuzzy sets and fuzzy inference is developed for a commercial adjustable damper. The proposed suspension system has also been simulated for various road profiles. Experiments are carried out to evaluate and compare the performance of traditional a PID controller and the proposed fuzzy control system for reducing vibration under a different experimental conditions for a quarter-car model. The experimental model and control algorithm will be described in the following sections.

## 2. MODEL OF SEMI-ACTIVE VIBRATION CONTROL IN A QUARTER-CAR SUSPENSION SYSTEM

The model of a semi-active quarter-car suspension system is shown in Fig. 2, where  $M_b$  and  $M_w$  denote the body mass and the wheel mass,  $X_b$  is the displacement of the vehicle body,  $X_w$  is the displacement of the tire,  $K_s$  is the coefficient of the

suspension spring,  $K_t$  is a tire spring with stiffness,  $X_r$  is the given road profile and  $F_d$  is the variable damping force of the shock absorber. According to dynamic analysis, the governing equation of a quarter car model can be obtained as

$$M_b \ddot{X}_b = -K_s(X_b - X_w) - F_d \quad (1)$$

$$M_w \ddot{X}_w = -K_s(X_b - X_w) - K_t(X_w - X_r) + F_d \quad (1)$$

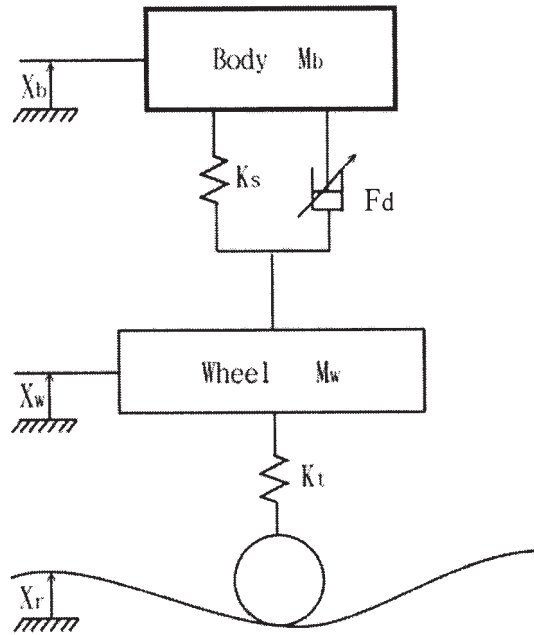


Figure 2. Quarter-car model of the semi-active suspension

In the present study, the vehicle mass  $M_b$  is 240 kg, tire mass  $M_w$  is 36 kg, the coefficient of the suspension spring  $K_s$  is 1400 N/m and the tire spring with stiffness  $K_t$  is 16,000 N/m. An adjustable damping mechanism is used for semi-active control to improve the response of the vehicle's dynamic behaviour. The force of this mechanism can be described as

$$F_d = C(\dot{X}_b - \dot{X}_w), \quad (3)$$

where  $C$  is the variable damping constant of the shock absorber,  $(\dot{X}_b - \dot{X}_w)$  is the relative velocity between the vehicle body and the tire. Using Eq. (3) to Eqs. (1) and (2), the equations of motion become

$$M_b \ddot{X}_b = -K_s(X_b - X_w) - C(\dot{X}_b - \dot{X}_w) \quad (4)$$

and

$$M_w \ddot{X}_w = K_s(X_b - X_w) - K_t(X_w - X_r) - C(\dot{X}_b - \dot{X}_w) \quad (5)$$

The system state variables are chosen by the equations of motion as follows

$$\begin{aligned} Z_1 &= X_b - X_w \\ Z_2 &= \dot{X}_b \\ Z_3 &= \dot{X}_w \\ Z_4 &= \ddot{X}_w \end{aligned} \quad (6)$$

## A Study of Semi-Active Vibration Control for Vehicle Suspension System Using an Adjustable Shock Absorber

Then, the equations of motion can be expressed as the following state space form

$$\dot{\underline{Z}} = \underline{A}\underline{Z} + \underline{B}\underline{X}_r \quad (7)$$

where

$$\underline{A} = \begin{bmatrix} 0 & 1 & 0 & -1 \\ -\frac{K_s}{M_b} & -\frac{C}{M_b} & 0 & \frac{C}{M_b} \\ 0 & 0 & 0 & 1 \\ \frac{K_s}{M_w} & \frac{C}{M_w} & -\frac{K_t}{M_w} & -\frac{C}{M_w} \end{bmatrix} \quad \underline{B} = \begin{bmatrix} 0 \\ 0 \\ 0 \\ \frac{K_t}{M_w} \end{bmatrix} \quad (8)$$

The dynamic responses of the semi-active suspension system are described in order to build the mathematical model. In order to obtain better dynamic responses, a PID controller and a fuzzy logic controller are designed for the mathematical model.

### 3. CONTROLLER DESIGN FOR A SEMI-ACTIVE SUSPENSION SYSTEM

#### 3.1 Road profile description

For good performance the semi-active suspension has to be adaptive all kinds of road conditions. Therefore, four road profiles are used in simulation of the quarter-car suspension model, there include sinusoidal, step, oscillation and random roads as shown in Fig. 3. The first input condition for testing the suspension system is a sinusoidal input signal of 60 mm amplitude for simulating a realistic hump road. The sinusoidal road profile is expressed as the following [11]

$$\underline{Z}_r(t) = Z_{\max} \cdot \sin\left(2\pi \frac{V_{\text{veh}}}{l_d} t\right) \quad , \quad 0 < t < \frac{l_d}{V_{\text{veh}}} \quad (9)$$

where  $Z_{\max}$  is the maximum displacement of the pulse,  $V_{\text{veh}}$  is the vehicle speed, and  $l_d$  is the displacement of the vibration. The second road profile input is a step that represents an abrupt change of road height of 80 mm. The step road profile is expressed as

$$\underline{Z}_r(t) = Z_{\max} \cdot \left[ 1 - e^{\left(-\pi \frac{V_{\text{veh}}}{l_d} t\right)} \cdot \left( 1 + \pi \cdot \frac{V_{\text{veh}}}{l_d} \cdot t \right) \right] \quad , \quad t > 0 \quad (10)$$

An oscillation road profile is the third input mat is similar to the macadam road. The oscillation road profile is expressed by the following equation

$$\underline{Z}_r(t) = 0.68684 Z_{\max} \left[ 1 - e^{\left(-0.25\pi \frac{V_{\text{veh}}}{l_d} t\right)} \cdot \left( \cos\left(\pi \frac{V_{\text{veh}}}{l_d} t\right) - \frac{1}{4} \sin\left(\pi \frac{V_{\text{veh}}}{l_d} t\right) \right) \right] \quad , \quad t > 0 \quad (11)$$

The final input uses a sinusoidal road profile with random noise. It likes to simulate a realistic macadam road. The random road profile is expressed as

$$\underline{Z}_r(t) = Z_{\max} \cdot \sin(\omega t + n) \cdot (u(t) - u(t-1)) \quad , \quad t > 0 \quad (12)$$

where  $Z_{\max} = 40$  mm and  $\omega = 1.88$  rad/sec and  $n$  is random number [10].

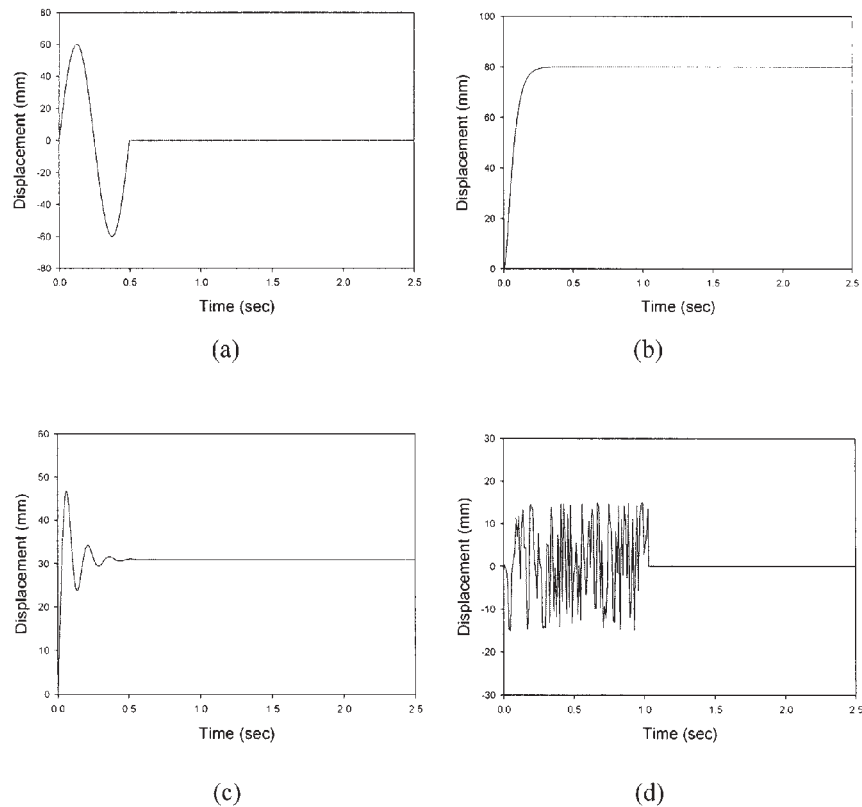


Figure 3. Various road conditions in simulation. (a) sinusoidal road profile (b) step road profile (c) oscillation road profile (d) random road profile

### 3.2 Design of fuzzy control system

A fuzzy logic control (FLC) that uses fuzzy sets and fuzzy inference to derive control laws for various road conditions is proposed in this section. In general, the FLC is more suitable for a complex system than other traditional controllers. The basic idea of FLC uses expert knowledge and experience to build a rule base with linguistic rules. Linguistic variables (SMALL, MEDIUM, LARGE, etc.) are used to represent the domain knowledge, with their membership value lying between 0 and 1.

The proposed FLC system is shown in Fig. 4. The fuzzy controller operation is typically divided into the following four categories:

- (a) Fuzzification: the fuzzification means that real values are translated in terms of fuzzy sets.
- (b) Rule design: a determination making logic to infer the FLC action based on the measured variables.
- (c) Inference engine: the control actions are encoded by means of fuzzy inference rules. The appropriate fuzzy sets are defined in the domains of the variable involved, and fuzzy logic operators and inference methods are formalised in computational terms.
- (d) Defuzzification: the results of the fuzzy computations are translated in terms of real values for the fuzzy control action.

In the present study, the input linguistic variables are body velocity (BV), and suspension velocity (SV). Body velocity has a set of three linguistic values which defined as:

$$BV = \langle\langle \text{Negative, Zero, Positive} \rangle\rangle$$

## A Study of Semi-Active Vibration Control for Vehicle Suspension System Using an Adjustable Shock Absorber

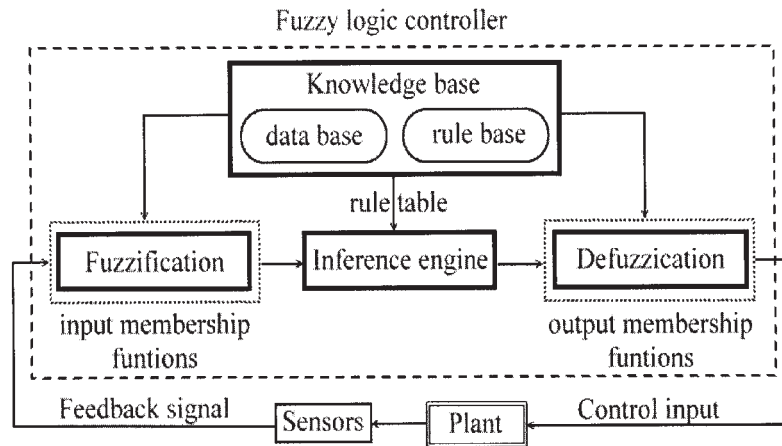


Figure 4. Structure of fuzzy control system

Suspension velocity has the same sets of linguistic values as body velocity. It can be written as:

$$SV = \langle\langle \text{Negative, Zero, Positive} \rangle\rangle$$

Moreover, the control signal (C) also has many linguistic values to provide different settings which can be firm, soft suspension or between. The linguistic values of the control signal set as

$$C = \langle\langle \text{Negative Soft, Positive Soft, Positive Firm, Negative Firm} \rangle\rangle$$

Gauss membership functions are used to represent the different linguistic variables for BV, SV and C. The membership functions of BV, SV and C are indicated in Fig. 5. The rule base is the critical part in designing the suspension controller because the rule base describes the control goals and control strategy of the domain experts by means of a set of linguistic control rules. In this work, each of the input variables has three linguistic values. Hence, there are nine possible cases. The rule base is developed by heuristics in Table I. The fuzzy logic control system provides better trade-off between ride comfort and road handling performance of the vehicle suspension system. In order to demonstrate the effect of the proposed fuzzy logic controller, a traditional PID controller was used in comparison of experimental work. The PID feedback control remains a very popular control strategy in many industrial processes. It can provide fast response, good system stability and small steady state errors in a linear system with known parameters. Three gains of PID controller are considered as adjustable parameters that change dynamic responses of the suspension system. The measurement of adjustable shock absorber and ride comfort assessment will be presented in following sections.

**Table I**  
Rule base for the fuzzy logic controller

	SV	N	Z	P
BV				
N		PS	PF	NF
Z		PS	PF	PF
P		NS	NF	PF

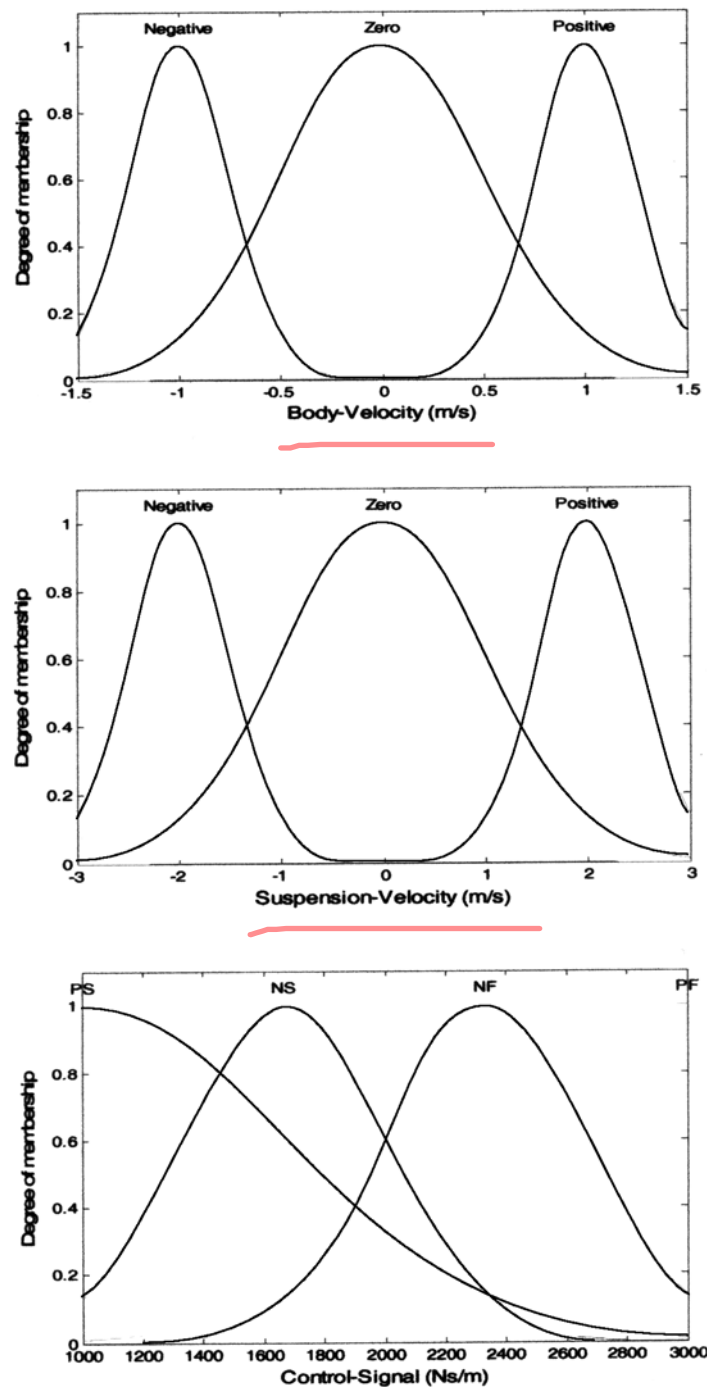


Figure 5. Membership function (a) body velocity; (b) suspension velocity; (c) control signal.

#### 4. MEASUREMENT OF THE ADJUSTABLE SHOCK ABSORBER

An adjustable damping system with 28 stages of damping selection is used for selecting the damping force by change the orifice valve of a double-tube hydraulic shock absorber. This enables the damping forces to be varied continuously in both expansion and compression. In the experimental investigation, the force and displacement are measured to evaluate the performance of the adjustable shock absorber. The complete experimental arrangement for measurement, including the load cell, a linear variable differential transformer (LVDT), a multi-conditioner cluster (MCC), an oscilloscope and data recording system. In order to measure the characteristic of the shock absorber, an AC motor rotates the eccentric applying

## A Study of Semi-Active Vibration Control for Vehicle Suspension System Using an Adjustable Shock Absorber

sinusoidal excitation at a fixed frequency in the shock absorber tester. The force and displacement signals are measured from the shock absorber tester in normal operating conditions. The excitation frequency is 1 Hz and the amplitude of excitation is 32 mm. The experimental arrangement to measure the shock absorber performance is shown in Fig. 6. In this study, the damping-force-adjustment of the adjustable shock absorber is discrete, not continuous. There are 28 stages of damping in the adjustable shock absorber. The measurement results of adjustable shock absorber in zero stage are shown in Fig. 7. The damping characteristics of the shock absorber are indicated by force-displacement (F-D) diagram and force-velocity (F-V) diagrams. The arrowheads in the figures represent the direction of the motion of the shock absorber. The damper demonstrated nonlinear response and hysteresis in the F-V diagram. This can be observed because the damping characteristics are obviously asymmetric and different between the extension and compression cycles of the F-D diagram. This hysteresis phenomenon means that the shock absorber produces the gap during the transition from compression to extension. Hence, the slope of the solid line is calculated in the F-V diagram for obtaining the optimum damping coefficient. The damping coefficient is about 996Ns/m for compression and 1354Ns/m for extension.

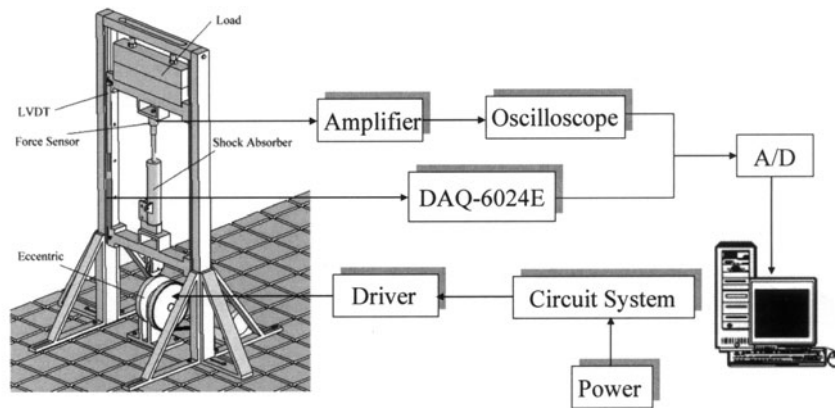


Figure 6. Experimental setup and measurement of shock absorber

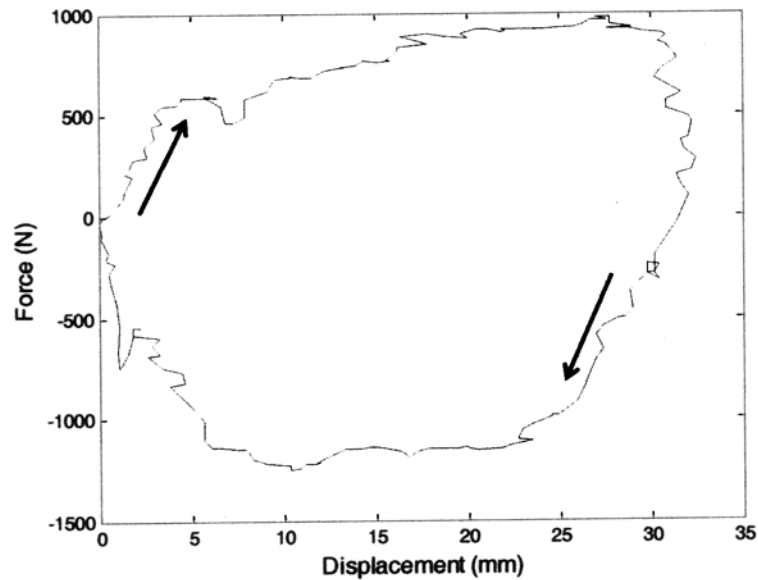
Comparison of the estimated performance at 1 Hz frequency and 32 mm amplitude for the various stages (settings) are shown in Fig. 8. The signals are measured at every third time stage of the 28 stages. The arrowheads in the figures represent the direction of the damping coefficient from low setting to high setting. It can be seen that the performance of the adjustable shock absorber except at the region of the velocity is near zero. Moreover, the damping coefficient characteristic of the adjustable shock absorber is summarised in Table II. The effect of adjustable settings stage on damping force is clearly shown in the table. Moreover, with the increasing of the setting stage, the damping force will increase considerably. From the measured results, it is concluded that the damping characteristics of commercial shock absorbers are nonlinear. Actually, the main features of the adjustable shock absorber can be described as follows:

- (a) It has asymmetric and nonlinear damping, lower damping coefficients for compression and higher damping coefficients for extension.
- (b) With changing of the setting stage, the damping force has is adjustable
- (c) The hysteresis is present

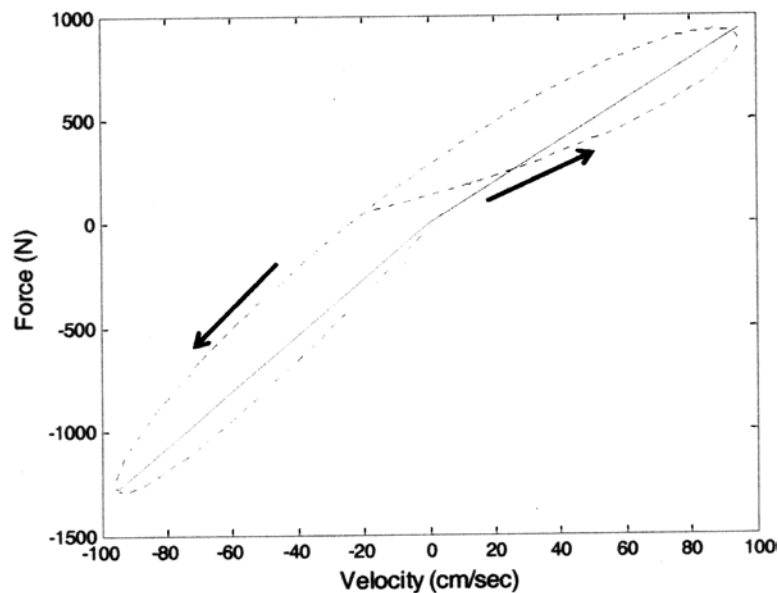


**Table II.**  
Damping coefficients of the adjustable shock absorber

Stage	Zero	3rd	6th	9th	12th	15th	18th
Damping coefficient							
$C_c$ (Ns/m)	996.85	987.41	1049.45	1054.56	1150.57	1207.31	1505.77
$C_e$ (Ns/m)	1354.66	1673.64	1703.6	1809.2	2025.32	2266.5	2480.6

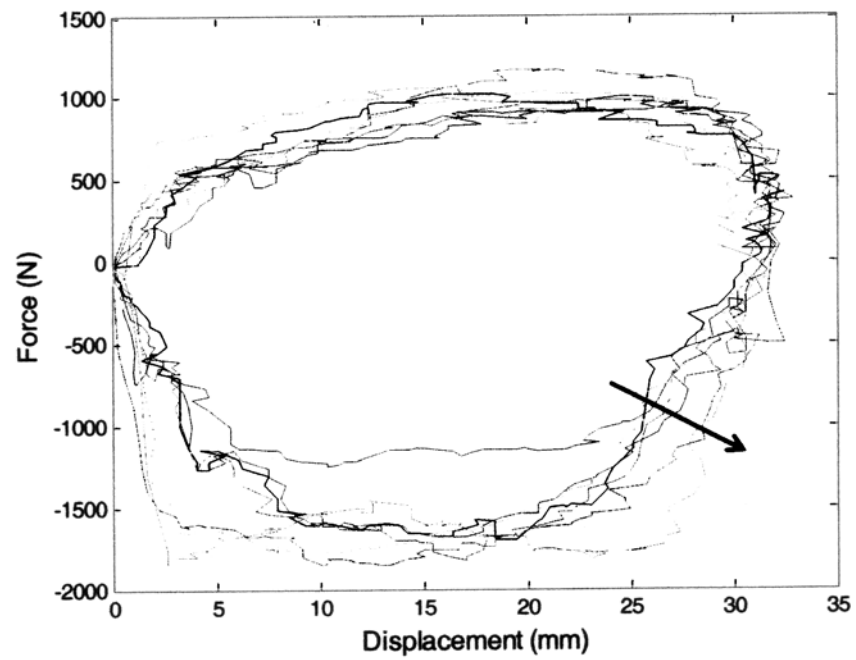


(a)

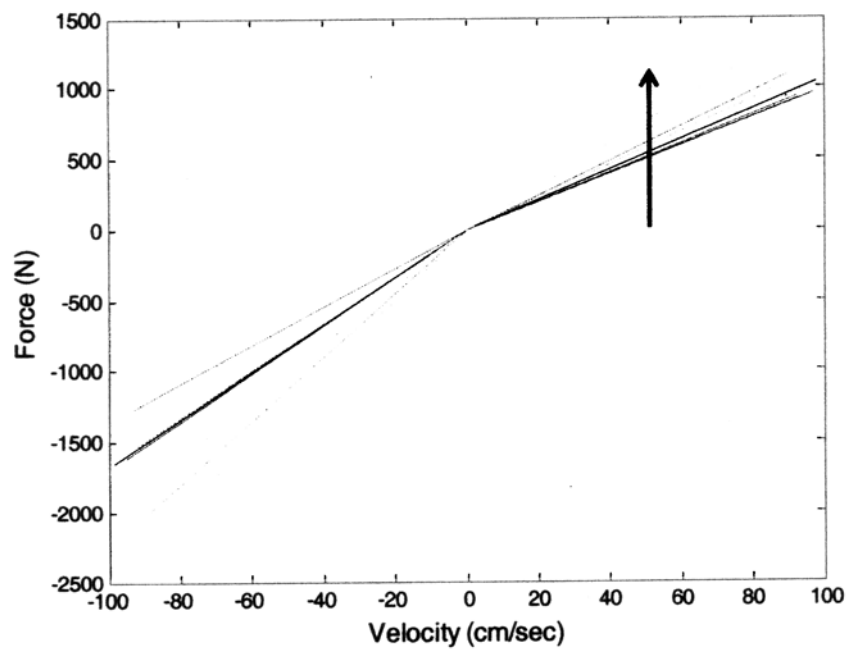


(b)

Figure 7. Characteristics of adjustable shock absorber in zero stage, the arrowheads means the direction of shock absorber. (a) force-displacement diagram (b) force-velocity diagram



(a)



(b)

Figure 8. Measurement results of adjustable shock absorber, the arrowheads represent the direction of the damping coefficient from low stage to high stages. (a) force-displacement diagram (b) force-velocity diagram

## 5. VEHICLE RIDE COMFORT ASSESSMENT

Vibration comfort is defined as the a reaction of a person to a vibration environment. Many drivers are exposed every day to mechanically induced vibration in their places of work. Therefore, it is very important to measure whole-body vibration in order to predict comfort. Because of the difficulty of evaluating response to vibration and inconsistencies in quantitative data obtained from research, the international standard ISO 2631-1 [12], for the evaluation of human exposure to whole-body vibration has been established. The standard provides numerical limits for exposure to vibration transmitted from solid surfaces to the human body in the frequency range of 1 to 80 Hz. It suggests that an equivalent acceleration magnitude is calculated using vibration measured in the back-to-chest direction (x-axis), right-to-left direction (y-axis) and vertical direction (z-axis) at the seat. Moreover, from one-third octave band frequency spectra (1-80Hz) of the frequency-weighted defined in International Standard 2631. Frequency weightings and multiplying factor for one third octave frequency spectrum (1-80 Hz) are defined in ISO 2631 for evaluating vibration with respect to ride comfort. It is found that comfort concerns are more likely if the vibration experienced is in the resonance zones which are 4-8 Hz for the z axis and 1-2 Hz for the x and y axes.

For evaluation of the vibration in a vehicle, ISO 2631-1 is used in the present study. Firstly, the vibration is calculated using weighted root-mean-square (RMS) acceleration that is defined as

$$a_w = \left[ \sum_i a_w(f_i)^2 \right]^{1/2}, \quad (13)$$

where  $a_w(f_i)$  is the weighted acceleration as a function of frequency and  $a_w$  is the weighted RMS acceleration. The total vibration value is obtained from the square root of the sum of the squares of the measured RMS ISO-weighted acceleration values in the x, y and z-directions. In health risk assessment, the weighted RMS value in each of the other two axes (x and y) are multiplied by 1.4. Therefore, the vector sum of the frequency-weighted RMS accelerations was calculated to evaluate the health risk from exposure to whole body vibration (WBV), as specified in ISO 2631-1, can be calculated as

$$a_v = (1.4a_{wx}^2 + 1.4a_{wy}^2 + a_{wz}^2)^{1/2} \quad (14)$$

Simultaneously, the vector sum of the frequency-weighted RMS accelerations was calculated to evaluate the ride comfort during exposure to WBV can be calculated as

$$a_v = (a_{wx}^2 + a_{wy}^2 + a_{wz}^2)^{1/2} \quad (15)$$

For comfort assessment, ISO 2631 provides a table that is an approximate indication of the likely reactions to various magnitudes of frequency-weighted RMS acceleration as shown in Table III. It is known that vibration magnitudes which produce RMS values in the region of 1 m/s<sup>2</sup> will commence cause discomfort. It is reasonable to suppose that increased exposure to vibration will be accompanied by increased risk of injury. This partial study introduces ISO 2631-1 which can be evaluated for vehicle ride comfort.

It focuses on the RMS value of three degree of freedom and is compared to the driver's vibration comfort assessment. The RMS values are determined by simulation of the response for various conditions and are reduced to improve the ride comfort by the designed controllers.

# A Study of Semi-Active Vibration Control for Vehicle Suspension System Using an Adjustable Shock Absorber

**Table III**

Likely reactions to various magnitudes of overall vibration total value

Vibration comfort	Frequency weighted acceleration ( m/s <sup>2</sup> , RMS)
Not uncomfortable	< 0.315
A little uncomfortable	0.315-0.63
Fairly uncomfortable	0.5-1
Uncomfortable	0.8-1.6
Very uncomfortable	1.25-2.5
Extremely uncomfortable	≥ 2

## 6. RESULTS AND DISCUSSION

For a quarter vehicle suspension system model, the dynamic equations are indicated in section 2. A sampling frequency of 100 Hz is selected in the simulating process. The simulation results of the semi-active suspension system using traditional PID and the proposed fuzzy control strategies are analysed and compared with the passive suspension system. They illustrate the effects of different controllers on the performance of the control systems. The proposed control systems were simulated and evaluated using different road profiles, such as sinusoidal, step, oscillation and random roads. The body displacement response of these road profiles for different controller is shown in Fig. 9. It can be observed the vehicle body stability conditions in different control methods and passive system. The body vertical acceleration of various road profiles for different controllers are shown in Fig. 10. It can be seen that the vertical acceleration represented the magnitude response of the vibration. In the present study, different suspension systems were evaluated as to their ability to reduce the effect of transient whole body vibrations. Spectra of measured vibrations displayed the energy distribution for different road profiles as shown in Fig. 11. In order to find the frequency-weighted acceleration values, the acceleration amplitude variations in the one-third octave band frequency spectra were represented as shown in Fig. 12.

In order to maintain with a compromise between driver comfort and ride safety, a good suspension control system has the RMS level less than high damping passive suspension system and a stability time shorter than low damping passive suspension system. Table IV show the RMS values of vertical acceleration (V.A.) and the stability time (S.T.) of vibration amplitude for high damping coefficient, low damping coefficient, semi-active with PID and semi-active with fuzzy logic

**Table IV**

RMS of vertical acceleration and the stability time of various road conditions

Road Response	Sinusoidal		Step		Oscillation		Random	
	V.A. RMS	S. T.	V.A. RMS	S. T.	V.A. RMS	S. T.	V.A. RMS	S. T.
Suspension								
Low Damping	1.05 (m/s <sup>2</sup> ) 78%	2.2 (sec)	0.63 (m/s <sup>2</sup> ) 81%	2 (sec)	0.63 (m/s <sup>2</sup> ) 70%	2 (sec)	0.84 (m/s <sup>2</sup> ) 80%	2.2 (sec)
High Damping	1.34 (m/s <sup>2</sup> ) 100%	1.4 (sec)	0.77 (m/s <sup>2</sup> ) 100%	1.2 (sec)	0.89 (sec) 100%	1 (sec)	1.04 (m/s <sup>2</sup> ) 100%	1.7 (sec)
PID Control	1.04 (m/s <sup>2</sup> ) 77%	1.9 (sec)	0.66 (m/s <sup>2</sup> ) 85%	1.5 (sec)	0.78 (m/s <sup>2</sup> ) 87%	1.9 (sec)	0.86 (m/s <sup>2</sup> ) 82%	2 (sec)
Fuzzy Control	1.09 (m/s <sup>2</sup> ) 81%	1.6 (sec)	0.63 (m/s <sup>2</sup> ) 81%	1.7 (sec)	0.71 (m/s <sup>2</sup> ) 79%	1.1 (sec)	0.82 (m/s <sup>2</sup> ) 78%	2.1 (sec)

suspension system for road profiles sinusoidal, step, oscillation and random respectively. It can be seen that the semi-active with fuzzy logic suspension system reduces average of the vertical acceleration by 20% compared with high damping suspension system. Furthermore, the stability time of vibration amplitude for fuzzy logic based system is less than 0.5 seconds compared with low damping suspension system. This means that fuzzy logic based system provides better ride quality and comfort as well as better road handling than other suspension systems.

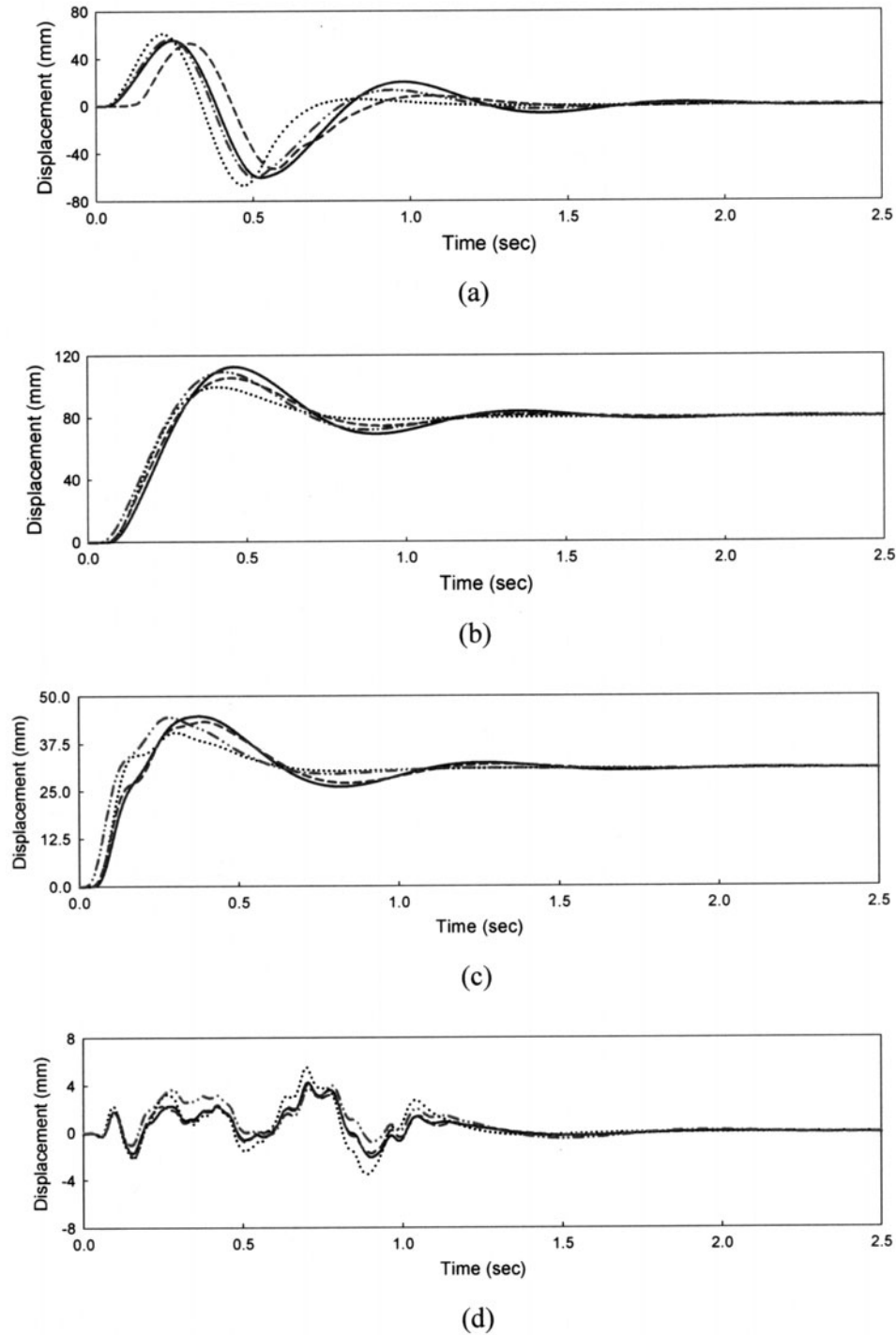
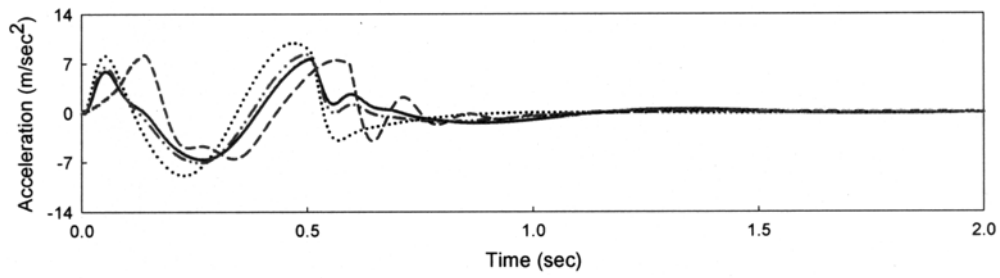
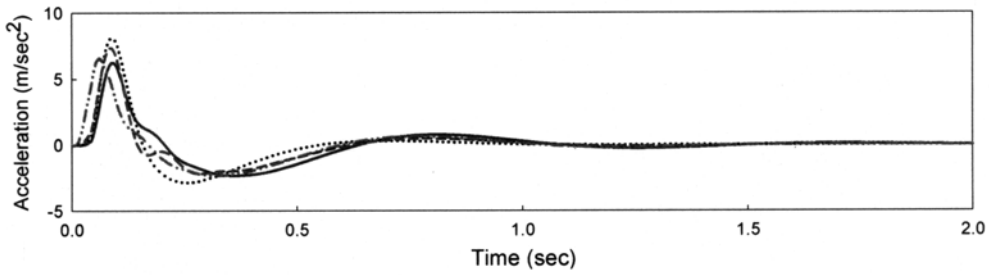


Figure 9. Body displacement response of different road profiles for different controller, high damping coefficient (point), low damping coefficient (solid), semi-active with PID controller (dotted), and semi-active with fuzzy controller (dashed) (a) sinusoidal road profile; (b) step road profile; (c) oscillation road profile; (d) random road profile.

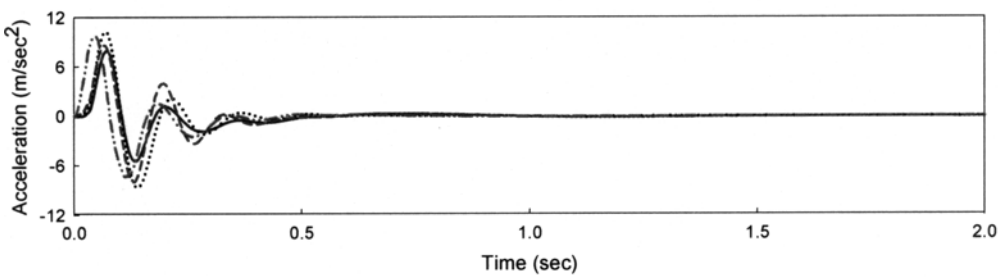
# A Study of Semi-Active Vibration Control for Vehicle Suspension System Using an Adjustable Shock Absorber



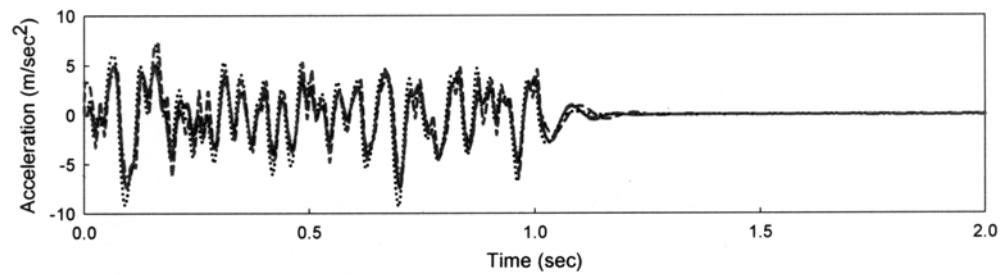
(a)



(b)



(c)



(d)

Figure 10. Body vertical acceleration of four road profiles for different controller implementation, high damping coefficient (solid), low damping coefficient (point), semi-active with PID controller (dashed), and semi-active with fuzzy controller (dotted). (a) sinusoidal road profile; (b) step road profile; (c) oscillation road profile; (d) random road profile.

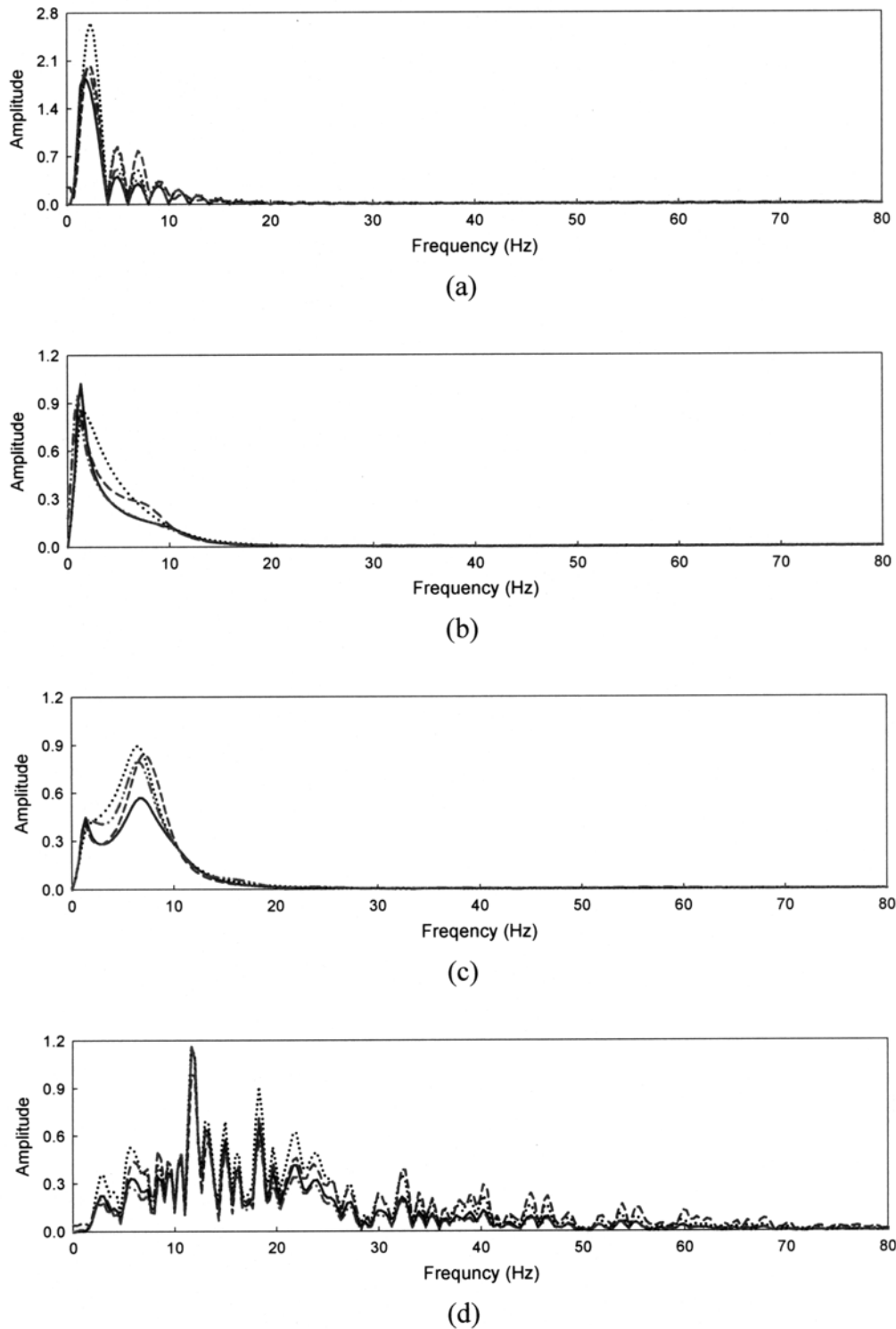


Figure 11. Spectrum of vibrations in the vertical direction (z-axis), high damping coefficient (point), low damping coefficient (solid), semi-active with PID controller (dotted), and semi-active with fuzzy controller (dashed). (a) sinusoidal road profile; (b) step road profile; (c) oscillation road profile; (d) random road profile.

## A Study of Semi-Active Vibration Control for Vehicle Suspension System Using an Adjustable Shock Absorber

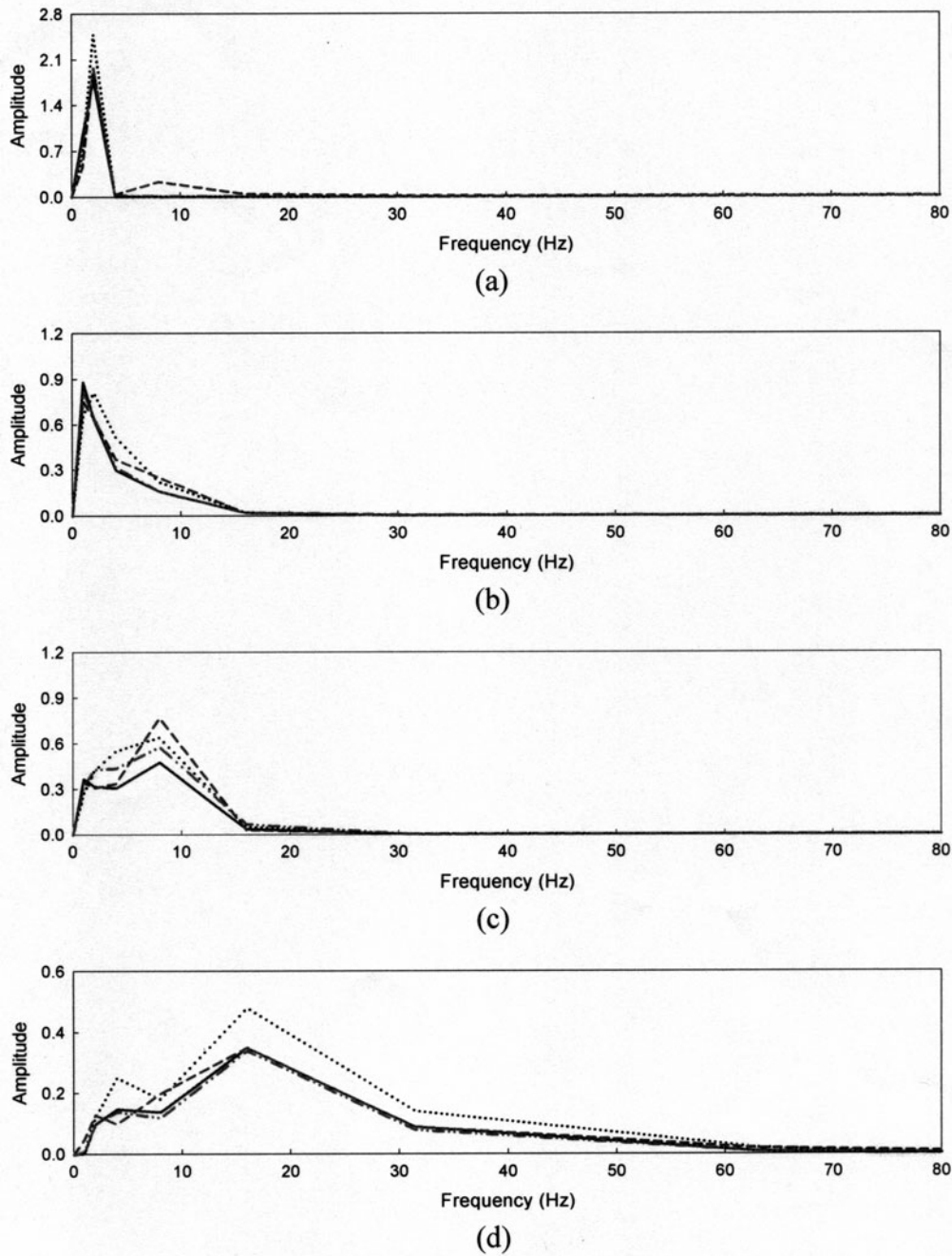


Figure 12. Acceleration amplitude variations in the one-third octave band frequency spectra, high damping coefficient (point), low damping coefficient (solid), semi-active with PID controller (dotted), and semi-active with fuzzy controller (dashed). (a) sinusoidal road profile; (b) step road profile; (c) oscillation road profile; (d) random road profile.

## 7. CONCLUSIONS

This paper describes a study of semi-active control for a quarter-car model. In the experimental investigation, the characteristic and performance of a vehicle shock absorber are measured for building a data bank for the simulation of response for various conditions. The dynamic control schemes for semi-active suspension are developed using a fuzzy logic controller. From the simulation results, the semi-active control provides lower RMS values and stability time of vibration amplitude than a passive suspension system. It demonstrates that the proposed controller achieves much better performance compared with passive suspension in various road conditions.



## ACKNOWLEDGEMENT

The study was supported by the National Science Council of Taiwan, the Republic of China, under project number NSC-94-2218-E-018-001.

## REFERENCES

1. Jackson, G W. *Fundamentals of the direct acting shock absorber*. SAE Paper 3712 National Passenger Car Body and Materials Meeting. 1959.
2. Satoh, M., Fukushima, N., & Akatsa, Y. An active suspension employing an electrohydraulic pressure control system. *The 29th IEEE International Conference on Decision and Control*. 1990, 4. 2226-2231.
3. Yao, G Z., Yap, F. F., Chen, G, Li, W. H., & Yeo, S. H. MR damper and its application for semi-active control of vehicle suspension system. *Mechatronics*. 2002. 12, 963-973.
4. Yildirim, S. Vibration control of suspension systems using a proposed neural network. *J Sound and Vibration*. 2004. 277(4), 1059-1069.
5. Al-Holou, N., Bajwa, A., & Joo, D. S. Computer controlled individual semi-active suspension system. *The 36th IEEE Midwest Symposium on Circuits and Systems*. 1993. 1. 208-211.
6. Al-Holou, N., Joo, D. S., & Shaout, A. The development of fuzzy logic based controller for semi-active suspension system. *The 37th IEEE Midwest Symposium on Circuits and Systems*. 1994, 2, 1373-1376.
7. Teramura, E., Haseda, S., Shimoyama, Y., Abe, T., & Matsuoka, K. Semi-active damping control system with smart actuator. *JSAE*. 1997, 18, 323-329.
8. Foda, S. G Fuzzy control of a quarter-car suspension system. *The 12th IEEE International Conference on Microelectronics*. 2000, 231 -234.
9. Rao, M. V. C., & Prahlad, V. A tunable fuzzy logic controller for vehicle-active suspension systems. *Fuzzy Sets and Systems*. 1997. 85. 11-21.
10. Joo, D. S., & Al-Holou, N. Development and evaluation of fuzzy logic controller for vehicle suspension systems. *The 27th IEEE Southeastern Symposium on System Theory*. 1995, 295-299.
11. Snowdon, J. C. Isolation from mechanical shock with a mounting system having nonlinear Dual-Phase damping. *The Shock and Vibration Bulletin* 41. 1970. 21-45.
12. International Organization for Standardization ISO 2631-1. Evaluation of human exposure to whole - body vibration, part 1: general requirements. *Mechanical Vibration and Shock*, Geneva, 1997.